MECSOL 2022 - Proceedings of the 8th International Symposium on Solid Mechanics
M.L. Bittencourt, J. Labaki, L.C.M. Vieira Jr. and E. Mesquita (Editors), Campinas SP, Brazil, October 17th to 19th, 2022

Topology Optimization Design of Acoustic-Poroelastic-Elastic Structures by the BESO Approach

Rodrigo L. Pereira[1] and Renato Pavanello[1]

[1] Department of Computational Mechanics, School of Mechanical Engineering, University of Campinas, Rua Mendeleyev 200, 13083-860 Campinas, Brazil

Porous materials are constantly the subject of study in the automotive and aerospace industries due to its sound insulation capabilities, lightweight characteristics, and vast degree of applicability, for example. Nevertheless, its mathematical formulations still pose a challenge, especially when topology optimization algorithms are considered, as multiphysics components must be contemplated for an enhanced degree of real-world simulation. In this work, the design of full modelled acoustic-poroelastic-elastic structures is formulated as a topology optimization problem. The Bi-directional Evolutionary Structural Optimization (BESO) algorithm is employed to offer non-intuitive design options with clearly defined boundaries. Biot's poroelasticity equations, expressed in the mixed $\mathbf{u}/p$ *form, and the Finite Element Method (FEM) comprise the basic expressions adopted in the description of all mediums and multiphysics interface conditions. With this unified multiphase (UMP) approach, it is possible to degenerate the poroelasticity expressions into the well-known scalar Helmholtz or elasto-dynamic equations, depending on the need for describing acoustic or elastic elements, respectively, without even implementing further coupling conditions. Additionally, this work also adopts a multiphase material interpolation scheme, which allows for systematic material changes, with only the elemental design variable information as input, and no boundary tracking. As Transmission Loss (TL) values are common indicators of the capability of a system in attenuate sound, the topology optimization problem is defined as the maximization of TL values at a specific target frequency. The proposed approach is tested through numerical examples that show the efficiency of the methodology.*
Keywords: Topology optimization, BESO method, Multiphysics, Porous materials

INTRODUCTION

Generally speaking, porous materials can be viewed as micro (or sometimes meso) perforated solid structures that are saturated with air. When this solid frame is considered to be montionless, the porous material can be modeled only with modifications of the scalar Helmholtz equation (Johnson et al., 1987; Champoux and Allard, 1991). For more real-life based simulations, however, the frame may be derived from an elastic component, hence having considerable displacements along its structure. In this case, complex multiphysical expressions are used to fully model the fluid-structure coupling of domains that presents such configuration.

As of 1956, Biot (1956a, 1956b) proposed expressions that were able to macroscopically describe the behavior of the wave in poroelastic materials, being mainly based on the displacements of the elastic and fluid components. Later in 1998, an even more suitable formulation was proposed by Atalla et al. (1998, 2001), which considered not only the displacements of the elastic frame, but also the interstitial pressure of the fluid component. This so called mixed $\mathbf{u}/p$ approach greatly reduced the Degrees of Freedom (dofs) involved in the Finite Element Method (FEM) implementation, being especially adopted in the works involving topology optimization procedures (Yamamoto et al., 2009; Lee et al., 2012, 2015, Hu et al. 2022).

Based on that, this work makes use of the Bi-directional Evolutionary Structural Optimization (BESO) method to maximize Transmission Loss (TL) values at a predefined target frequency. The investigated domains are mainly composed of poroelastic materials, represented by the mixed $\mathbf{u}/p$ formulation, but with the possibility of degeneration to acoustic or elastic elements by means of the unified multiphase (UMP) approach (Lee, 2009; Lee et al., 2012). In this sense, multiphysical aspects compose the optimization, as acoustic-poroelastic-elastic domains interact throughout the entire procedure. In a systematic way, these components are rearranged in each iteration, in accordance with the adopted multiphase material interpolation scheme.

THE MIXED U/P FINITE ELEMENT FORMULATION FOR POROELASTIC MEDIA

Assuming that the porous material properties are homogeneous and subject to harmonic osculations ($e^{j\omega t}$), the mixed displacement-pressure ($\mathbf{u}/p$) formulation may be written in the following form,

$$\nabla \cdot \hat{\underline{\boldsymbol{\sigma}}}^s + \omega^2 \tilde{\rho}\mathbf{u} + \tilde{\gamma}\nabla p = \mathbf{0}, \tag{1}$$

$$\nabla^2 p + \omega^2 \frac{\tilde{\rho_{22}}}{\tilde{R}} p - \omega^2 \frac{\tilde{\rho_{22}}}{\phi^2}\tilde{\gamma}\nabla \cdot \mathbf{u} = 0, \tag{2}$$

where ∇ is the gradient operator, ∇^2 is the Laplace operator, ω is the angular frequency, $j^2 = -1$ is the imaginary unit, t is time, $\mathbf{u}$ is the solid phase displacement, p is the interstitial pressure and ϕ is the porosity. The combined effective density $\tilde{\rho}$ and coupling coefficient $\tilde{\gamma}$ are defined as,

$$\tilde{\rho} = \tilde{\rho}_{11} - \frac{\tilde{\rho}_{12}^2}{\tilde{\rho}_{22}}, \quad \tilde{\gamma} = \phi\left(\frac{\tilde{\rho}_{12}}{\tilde{\rho}_{22}} - \frac{\tilde{Q}}{\tilde{R}}\right), \tag{3}$$

with $\tilde{\rho}_{11}$, $\tilde{\rho}_{22}$, $\tilde{\rho}_{12}$ being the effective densities that account for the inertia effects in the solid, fluid and in the viscous coupling that happens between the two, respectively. The stress tensor of the porous material in vacuo $\hat{\underline{\boldsymbol{\sigma}}}^s$ has also a mathematical expression associated to it,

$$\hat{\underline{\boldsymbol{\sigma}}}^s = \left(\tilde{A} - \frac{\tilde{Q}^2}{\tilde{R}}\right)\nabla \cdot \mathbf{u}\mathbf{I} + 2N\underline{\boldsymbol{\varepsilon}}^s = \hat{A}\nabla \cdot \mathbf{u}\mathbf{I} + 2N\underline{\boldsymbol{\varepsilon}}^s, \tag{4}$$

where $\mathbf{I}$ is the identity tensor, $\underline{\boldsymbol{\varepsilon}}^s$ is the solid phase strain tensor, $\tilde{A}$ is the first Lamé constant of the poroelastic material, N is the elastic shear modulus, $\tilde{Q}$ is the coupling coefficient between the dilatation of both component phases, $\tilde{R}$ is the bulk modulus of air occupying a fraction of volume aggregate and $\hat{A}$ is the first Lamé constant of the elastic phase in vacuo (Atalla et al., 1998; Lee et al. 2015).

The weak form of Eqs. (1) and (2) is then obtained by the combination of the Weighted Residuals Method and the divergence theorem, followed by the consideration of material isotropy, that is (Rigobert et al., 2003; Lee et al. 2015),

$$\int_{\Omega_p} \left\{ \hat{\underline{\boldsymbol{\sigma}}}^s(\mathbf{u}) : \underline{\boldsymbol{\varepsilon}}^s(\delta\mathbf{u}) - \omega^2\tilde{\rho}\mathbf{u}\cdot\delta\mathbf{u} - (\tilde{\gamma}+\tilde{\xi})\nabla p\cdot\delta\mathbf{u} - \tilde{\xi}p\nabla\cdot\delta\mathbf{u} \right\} d\Omega_p - \int_{\Gamma_p} (\underline{\boldsymbol{\sigma}}^t \cdot \mathbf{n})\cdot\delta\mathbf{u}\, d\Gamma_p = \mathbf{0}, \tag{5}$$

$$\int_{\Omega_p} \left\{ \frac{\phi^2}{\omega^2\tilde{\rho}_{22}}\nabla p\cdot\nabla\delta p - \frac{\phi^2}{\tilde{R}}p\delta p - (\tilde{\gamma}+\tilde{\xi})\nabla\delta p\cdot\mathbf{u} - \tilde{\xi}\delta p\nabla\cdot\mathbf{u} \right\} d\Omega_p - \int_{\Gamma_p} \phi(\mathbf{U}-\mathbf{u})\cdot\mathbf{n}\delta p\, d\Gamma_p = 0, \tag{6}$$

where $\delta\mathbf{u}$ and δp are test functions related with the solid phase displacement and the interstitial pressure, respectively, while Ω_p represents the poroelastic domain with Γ_p as its boundary. The newly introduced variable $\tilde{\xi} = \phi(1+\tilde{Q}/\tilde{R})$ may be also viewed as a coupling coefficient, and $\mathbf{n}$ is the outward unit normal vector.

An important point is that Eqs. (5) and (6) have boundary related expressions that can be physically specified on the interface of two distinct poroelastic media, that is the traction vector, $\underline{\boldsymbol{\sigma}}^t \cdot \mathbf{n}$, and the relative displacement vector, $(\mathbf{U}-\mathbf{u})\cdot\mathbf{n}$. Joining this characteristic with the continuity of the nodal variables that it is common to the FEM, the coupling of poroelastic-poroelastic and poroelastic-elastic materials happens naturally and completely free of further approximations (Atalla et al., 2001).

The FEM is then considered in the discretization of the aforementioned continuous problem, being also followed by Galerkin's approach. The result is a linear system of equations (Allard and Atalla, 2009), as can be seen next,

$$\begin{bmatrix} \mathbf{K}-\omega^2\tilde{\mathbf{M}} & -(\tilde{\mathbf{C}}_1+\tilde{\mathbf{C}}_2) \\ -(\tilde{\mathbf{C}}_1+\tilde{\mathbf{C}}_2)^T & \tilde{\mathbf{H}}/\omega^2 - \tilde{\mathbf{Q}} \end{bmatrix} \begin{Bmatrix} \mathbf{u} \\ \mathbf{p} \end{Bmatrix} = \begin{Bmatrix} \mathbf{f}_s \\ \mathbf{f}_p/\omega^2, \end{Bmatrix}, \tag{7}$$

where $\mathbf{K}$, $\tilde{\mathbf{M}}$, $\tilde{\mathbf{H}}$, $\tilde{\mathbf{Q}}$, $\tilde{\mathbf{C}}_1$, $\tilde{\mathbf{C}}_2$ denote the global stiffness, mass, kinetic, compression and coupling matrices, respectively. The global displacement and acoustic pressure vectors, as well as the global structural and acoustic loads are respectively defined as $\mathbf{u}$, $\mathbf{p}$, $\mathbf{f}_s$, $\mathbf{f}_p$.

UNIFIED MULTIPHASE MODELING APPROACH

Following the works of Lee (2009) and Lee et. al (2012), the UMP approach aims at using Biot's equations, in the $\mathbf{u}/p$ form, to easily describe the three main medias considered in vibroacoustic systems applications. Hence, the scalar

Helmholtz and the elasto-dynamic equations are directly derived from Eqs. (1) and (2) if ones goal is to simulate acoustic or elastic materials, respectively. This happens by taking limit values of some material parameters, in order to degenerate the original Biot's equations in the ones of interest. As a direct consequence of the method, no boundary tracking is ever needed when changing from one element type to another.

In a numerical point of view, six variables are directly controlled by the UMP approach, in a way that the dynamic properties of the base poroelastic material are changed in accordance with the element configuration. In a purely poroelastic scenario, the variables are: $\tilde{\xi}$, $\tilde{\rho}$, N, $\hat{A}$, $\phi^2/\tilde{\rho}_{22}$ and $\phi^2/\tilde{R}$. For the acoustic case, the same variables assume the following form: 1, 0, 0, 0, $1/\rho_a$ and $1/\kappa_a$, where κ_a is the bulk modulus of the air (identified by the subscript a). Lastly, for the elastic case, one gets the sequence: 0, ρ_e, N_e, $\tilde{A}_e$, 0 and 0, with the subscript e being related with the elastic material.

A downside of this approach, in a finite element point of view, regards the singularity that happens when completely canceling one of the aforementioned variables. To solve this issue, small valued coefficients are assigned to each of the properties that have to be zero, in a way that all the sequences get the following results,

$$\{\tilde{\xi},\tilde{\rho},N,\hat{A},(\phi^2/\tilde{\rho}_{22}),(\phi^2/\tilde{R})\}_p = \{\tilde{\xi},\tilde{\rho},N,\hat{A},\phi^2/\tilde{\rho}_{22},\phi^2/\tilde{R}\}, \tag{8}$$

$$\{\tilde{\xi},\tilde{\rho},N,\hat{A},(\phi^2/\tilde{\rho}_{22}),(\phi^2/\tilde{R})\}_a = \{1,\varepsilon_a\tilde{\rho},\varepsilon_a N,\varepsilon_a\hat{A},1/\rho_a,1/\kappa_a\}, \tag{9}$$

$$\{\tilde{\xi},\tilde{\rho},N,\hat{A},(\phi^2/\tilde{\rho}_{22}),(\phi^2/\tilde{R})\}_e = \{\varepsilon_e\tilde{\xi},\rho_e,N_e,\tilde{A}_e,\varepsilon_e(\phi^2/\tilde{\rho}_{22}),\varepsilon_e(\phi^2/\tilde{R})\}, \tag{10}$$

with the subscript p referring to the poroelastic materials. In this work, the values of ε_a and ε_e were carefully selected to be 1×10^{-4} and 1×10^{-9}, respectively.

Material interpolation scheme: acoustic, elastic and poroelastic relations

As the main objective of this paper is to study the design of structures composed of acoustic-poroelastic-elastic medias, a multiphase material interpolation scheme is presented in Eqs. (11) to (16) with the goal of providing systematic material changes along the entire optimization process,

$$\tilde{\xi} = \tilde{\xi}_e + x_2^{\zeta_2}(\tilde{\xi}_p - \tilde{\xi}_e) + x_1^{\zeta_1}(\tilde{\xi}_a - \tilde{\xi}_p), \tag{11}$$

$$\tilde{\rho} = \tilde{\rho}_e + x_2^{\zeta_2}(\tilde{\rho}_p - \tilde{\rho}_e) + x_1^{\zeta_1}(\tilde{\rho}_a - \tilde{\rho}_p), \tag{12}$$

$$N = N_e + x_2^{\zeta_2}(N_p - N_e) + x_1^{\zeta_1}(N_a - N_p), \tag{13}$$

$$\hat{A} = \hat{A}_e + x_2^{\zeta_2}(\hat{A}_p - \hat{A}_e) + x_1^{\zeta_1}(\hat{A}_a - \hat{A}_p), \tag{14}$$

$$\phi^2/\tilde{\rho}_{22} = (\phi^2/\tilde{\rho}_{22})_e + x_2^{\zeta_2}[(\phi^2/\tilde{\rho}_{22})_p - (\phi^2/\tilde{\rho}_{22})_e] + x_1^{\zeta_1}[(\phi^2/\tilde{\rho}_{22})_a - (\phi^2/\tilde{\rho}_{22})_p], \tag{15}$$

$$\phi^2/\tilde{R} = (\phi^2/\tilde{R})_e + x_2^{\zeta_2}[(\phi^2/\tilde{R})_p - (\phi^2/\tilde{R})_e] + x_1^{\zeta_1}[(\phi^2/\tilde{R})_a - (\phi^2/\tilde{R})_p], \tag{16}$$

where $x_{1,2}$ represent the design variables and the superscripts $\zeta_{1,2}$ are the penalty coefficients. At this stage, it is important to note that even thought the elastic and acoustic materials are indeed degenerated poroelastic ones, as highlighted in Eqs. (8), (9) and (10), comparisons between the UMP approach and the segregated formulations (scalar Helmholtz for acoustic, elasto-dynamic for elastic and Biot's equations for poroelastic) have been conducted by the authors, hence validating the current numerical approach. Another notable point is that, after a series of test, the following values were chosen for the design variables,

$$\{x_1,\ x_2\} = \{1,\ 1\}, \qquad \text{for acoustic elements,} \tag{17}$$

$$\{x_1,\ x_2\} = \{x_{\min},\ 1\}, \qquad \text{for poroelastic elements,} \tag{18}$$

$$\{x_1,\ x_2\} = \{x_{\min},\ x_{\min}\}, \qquad \text{for elastic elements,} \tag{19}$$

and for the penalty variables, $\{\zeta_1,\ \zeta_2\} = \{2,\ 1\}$. The user defined $x_{\min} = 0.001$ parameter is the lower limit that the design variable can get, being usually adopted to avoid numerical singularities. Finally, the poroelastic and elastic material properties adopted in this work are presented in Table 1, while the acoustic ones are the same as brought by Pereira et al. (2022).

Table 1 – Poroelastic and elastic material properties (Yamamoto et al. 2009)

Parameters	Polyurethane foam	Olefin sheet
Porosity ϕ	0.97	–
Tortuosity α_∞	2.5	–
Static flow resistivity σ (N s m^{-4})	7×10^4	–
Viscous characteristic length Λ (μm)	36×10^{-6}	–
Thermal characteristic length Λ' (μm)	170×10^{-6}	–
Solid mass density ρ (kg m^{-3})	1433	1790
Young's modulus E (Pa)	2.67×10^5	1.75×10^8
Poisson ratio ν	0.4	0.4
Loss factor η	0.11	0.205

TOPOLOGY OPTIMIZATION FORMULATION

Since TL values are common vibroacoustic indicators regarding the attenuation of sound in acoustic systems, the topology optimization problem here investigated aims at the maximization of TL values at target frequencies, when subjected to equilibrium equations (Eq. 7) and volume constraints,

$$\text{Maximize: } \mathrm{TL} = 20\log_{10}\left(\left|\frac{1}{p_3}\frac{p_1 - p_2\exp(-jk_aL)}{1-\exp(-j2k_aL)}\right|\right), \tag{20}$$

$$\text{Subjected to: } \begin{cases} \begin{bmatrix} \mathbf{K}-\omega^2\tilde{\mathbf{M}} & -(\tilde{\mathbf{C}}_1+\tilde{\mathbf{C}}_2) \\ -(\tilde{\mathbf{C}}_1+\tilde{\mathbf{C}}_2)^T & \tilde{\mathbf{H}}/\omega^2-\tilde{\mathbf{Q}} \end{bmatrix} \begin{Bmatrix} \mathbf{u} \\ \mathbf{p} \end{Bmatrix} = \begin{Bmatrix} \mathbf{f}_s \\ \mathbf{f}_p/\omega^2, \end{Bmatrix}, \\ \begin{Bmatrix} V_1^* - \left(\sum_{i=1}^{N_{\mathrm{el}}} V_i\gamma_i\right)_1 \\ V_2^* - \left(\sum_{i=1}^{N_{\mathrm{el}}} V_i\gamma_i\right)_2 \end{Bmatrix} = \begin{Bmatrix} 0 \\ 0 \end{Bmatrix}, \\ \underline{\mathbf{x}} = \left[\begin{Bmatrix} x_1 \\ \vdots \\ x_{N_{\mathrm{el}}} \end{Bmatrix}_1, \begin{Bmatrix} x_1 \\ \vdots \\ x_{N_{\mathrm{el}}} \end{Bmatrix}_2\right]. \end{cases} \tag{21}$$

As observed in Eq. (20), the two sound pressure amplitudes that are collected at the left side of the system (inlet) are p_1 and p_2, apart L from each other, while the one gathered at the right side (outlet) is p_3 (see Fig. 1). Here, the wave number is denoted as k_a. In Eq. (21) the prescribed final volume fraction is V^*, with the design domain volume fraction being $\sum_{i=1}^{N_{\mathrm{el}}} V_i\gamma_i$. N_{el} is the number of elements of the entire porous domain and $\underline{\mathbf{x}}$ is the design variable matrix. The subscript numbers 1 and 2 represents the changes that happens along the optimization process, in other words, the number 1 refers to variations from acoustic to poroelastic elements, while the number 2 regards the changes from poroelastic to elastic. It is remarked, however, that changes from acoustic to poroelastic happens prior to poroelastic to elastic, in a way that the final volume fraction of poroelastic materials have to be achieved to start the next set of alterations (poroelastic to elastic). Finally, it may also be noted that once V_1^* is reached, the value is kept constant until the achivement of V_2^* (Huang and Xie, 2010).

Sensitivity analysis

As previously highlighted, TL values are often observed when dealing with acoustic systems, which motivated many researchers to conduct the derivation of Eq. (20) (Lee, 2009; Yoon, 2013; Lee et al. 2015; Azevedo et al., 2018; Ferrándiz et al. 2020; Hu et al., 2022). In a mathematical perspective, the elemental sensitivity number, α_i, is usually obtained as,

$$\alpha_i = \frac{\partial \mathrm{TL}}{\partial x_i} = \frac{10}{\ln 10}\left(\frac{\partial|p_{\mathrm{in}}|^2}{\partial x_i}\frac{1}{|p_{\mathrm{in}}|^2} - \frac{\partial|p_{\mathrm{out}}|^2}{\partial x_i}\frac{1}{|p_{\mathrm{out}}|^2}\right), \tag{22}$$

where,

$$|p_{\text{in}}| = |(p_1 - p_2\, e^{-jk_aL})/(1 - e^{-j2k_aL})| \tag{23}$$

$$|p_{\text{out}}| = |p_3|. \tag{24}$$

After open the expressions for $\partial|p_{\text{in}}|^2/\partial x_i$ and $\partial|p_{\text{out}}|^2/\partial x_i$, one will need to find the partial derivatives of the observed pressures in the jth node, hence,

$$\frac{\partial p_j}{\partial x_i} = -\hat{\mathbf{p}}_j^T \begin{bmatrix} \dfrac{\partial \mathbf{K}}{\partial x_i} - \omega^2 \dfrac{\partial \tilde{\mathbf{M}}}{\partial x_i} & -\left(\dfrac{\partial \tilde{\mathbf{C}}_1}{\partial x_i} + \dfrac{\partial \tilde{\mathbf{C}}_2}{\partial x_i}\right) \\ -\left(\dfrac{\partial \tilde{\mathbf{C}}_1}{\partial x_i} + \dfrac{\partial \tilde{\mathbf{C}}_2}{\partial x_i}\right)^T & \dfrac{1}{\omega^2}\dfrac{\partial \tilde{\mathbf{H}}}{\partial x_i} - \dfrac{\partial \tilde{\mathbf{Q}}}{\partial x_i} \end{bmatrix} \begin{Bmatrix} \mathbf{u} \\ \mathbf{p} \end{Bmatrix}, \tag{25}$$

where,

$$\hat{\mathbf{p}}_j^T = \mathbf{f}_j^T \begin{bmatrix} \mathbf{K} - \omega^2 \tilde{\mathbf{M}} & -(\tilde{\mathbf{C}}_1 + \tilde{\mathbf{C}}_2) \\ -(\tilde{\mathbf{C}}_1 + \tilde{\mathbf{C}}_2)^T & \tilde{\mathbf{H}}/\omega^2 - \tilde{\mathbf{Q}} \end{bmatrix}^{-1}, \tag{26}$$

being the solution of the transposed problem. The partial derivatives resulted from Eq. (25) are easily obtained from the material interpolation schemes provided in Eqs. (11) to (16). Finally, $\mathbf{f}_j$ may be viewed as a locator, that is a vector full of zeros, except on the dof referred to p_j.

Overview of the BESO method

The BESO method is the topology optimization approach of choice in this work, as proposed by Huang and Xie (2010), since it provides clearly defined designs at all stages of the iterative problem. The following algorithm summarizes the entire method.

Algorithm 1: BESO algorithm

Input: Define geometry and FEM parameters
Define BESO parameters: $\underline{\mathbf{x}}$, V^*, $\mathrm{r_{min}}$, ER, $\mathrm{AR_{max}}$, $\zeta_{1,2}$
Evaluate **u** and **p**
Start iteration counter: $r = 0$
while $err < 0.005$ ***or*** $V_1^{(r)} + V_2^{(r)} \neq V_1^* + V_2^*$ **do**
  $r = r + 1$
  Calculate sensitivity numbers
  Filter sensitivities (+ historical averaging + normalization)
  Update design domain
  Update volume domain
  Evaluate **u** and **p**
  Evaluate TL

$$err = \frac{|\sum_{b=1}^{10} \mathrm{TL}^{(r-b+1)} - \sum_{b=1}^{10} \mathrm{TL}^{(r-9-b)}|}{\sum_{b=1}^{10} \mathrm{TL}^{(r-b+1)}} \leq 0.005 \tag{27}$$

Output: Optimized topology

In Algorithm 1, it is perceptive that the domain geometry needs to be known beforehand, as well as the solution vectors **u** and **p**. Next, in the while loop, the sensitivities are calculated and then filtered, following a projection approach that is controlled by the filter radius, r_{rmin}. To increase the stability of the optimization, two more procedures are commonly performed, being the historical averaging of the elemental sensitivities and its normalization (Zhou et al., 2021). Before updating the design variables, it is necessary to first determine the volume of the next iteration, $V^{(r+1)}$, with the information of the current, $V^{(r)}$, and the Evolutionary Rate (ER), that is $V^{(r+1)} = V^{(r)}(1 \pm \mathrm{ER})$.

The sensitivity numbers are then sorted from highest to lowest, in order to assign the elements with the biggest α_i values as "full" and the smallest as "void". The bi-directionality of the BESO approach is characterized by the allowance

of the contrary mechanism, that is "void" elements can turn back to be "full", which is controlled by the Addition Ratio (AR_{max}). As the topology is updated, the solution vectors **u** and **p** are obtained, followed by the transmission loss values. The final step is done by the calculation of the iteration error, that has to be smaller then the tolerance of 0.5%.

NUMERICAL EXAMPLES

In this section the optimization of two distinct systems composed of acoustic-poroelastic-elastic components are presented and discussed. Figure 1 shows two fairly similar systems, but with different boundary conditions. In the first one, shown in Fig. 1 (a), the top surface is considered to be a hard wall (all elastic dofs are blocked), while the bottom is a symmetry boundary (only the dofs in the y direction are blocked). A pressure imposed plane wave enters at the left side of the system, while an anechoic termination is considered to be present at the far right. It is remarked that, in all domains here considered, only poroelastic elements exist, being therefore modified to represent acoustic or elastic elements by the UMP technique. In this sense, all nodes have three dofs, even when they are in the "modified form", where two are related with the displacements of the elastic frame and one with the interstitial pressure. As a consequence, the imposition of the boundary conditions here considered are not straightforward, being presented in detail in the works of Lee (2009) and Lee et al. (2012).

Still in Fig. 1 (a), the design domain, Ω_d, is characterized by a light grey area of 8x5 cm^2, and the non-design domain, Ω_{nd}, by two white and small black areas of 1x5 cm^2 and 0.1x5 cm^2, respectively. Three previously chosen points of observation of pressure (inside inverted triangles) are also present. Figure 1 (b) shows the same elements as previously highlighted, but with symmetry boundary conditions also in the top surface of the system. Another common fact regarding both scenarios is the number of finite elements. It is a known fact that to simulate poroelastic structures more elements are required per wavelength then common acoustic ones. Based on this, the entire system is composed of 102 x 40 first order quadrilateral elements, being way above the recommended per wavelength (Atalla and Sgard, 2015).

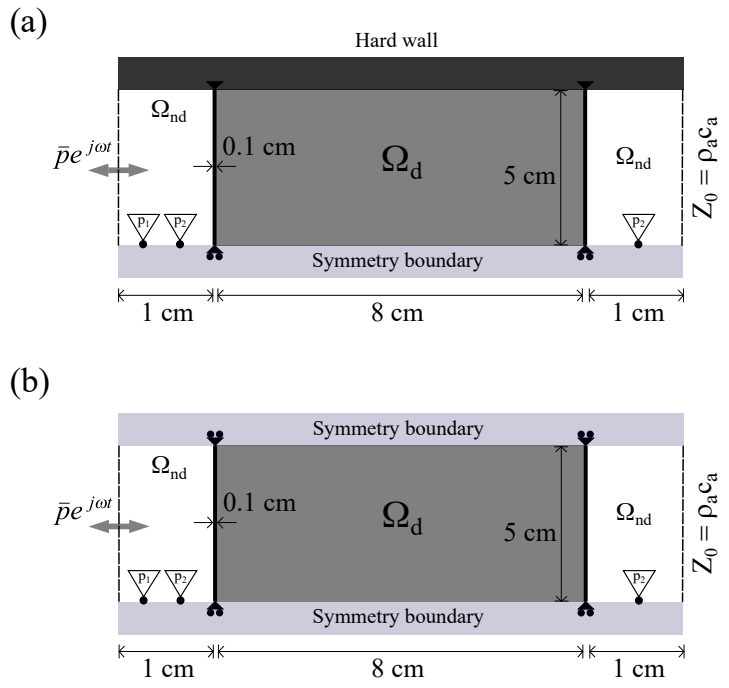

Figure 1 – Details of the geometries investigated.

In this study, the initial configuration is that acoustic elements fill the entire Ω_d (light grey area), while Ω_{nd} has both, acoustic (white areas) and elastic (black area) components. In this sense, the BESO parameters are chosen to be ER = 1%, AR = 0.5%, r^1_{min} = 3 cm and r^2_{min} = 2 cm. These two distinct filter radius were adopted as an effort to reduced isolated configurations throughout the design domain. Furthermore, V_1^* and V_2^* assume the values of 0.5 and 0.05, respectively, which guarantees that porous materials occupy 50% of the design domain, while the elastic component fills 5% of it. For the sake of conciseness, the scenarios shown in Figs. 1 (a) and (b) will be referred, from now on, as Hard-Symmetry (or simply HS) and Symmetry-Symmetry (SS).

Topology Optimization of the Hard-Symmetry and Symmetry-Symmetry systems

Figure 2 shows the main results obtained from the analysis of the HS system (see Fig. 1 (a)) for the target frequency of 250 Hz. In Fig. 2 (b), the evolution of the volume fractions for acoustic (Vol.Frac - A), poroelastic (Vol.Frac - P) and elastic (Vol.Frac - E) components are shown, together with the behavior of the objective function along the iterative procedure. It is perceptive that TL values vary greatly throughout the course of the optimization, in a way that the procedure stops only due to the mean values obtained in the calculation of Eq. (27). This fact shows that the ER and ARmax values chosen need to be reevaluated to an even lower number, as an effort to reduce such erratic behavior.

Nevertheless, the topology resulted seem to be effective in promoting the increase of TL values, not only in the target frequency, but also in the vast range of frequencies observed. Besides, the choice of different filter radius sizes is here justified, as the poroelastic-elastic structures appear quite close to each other, instead of generating expressive material disconnections (like porous structures floating on air); enhancing the manufacturability of the global optimized topologies.

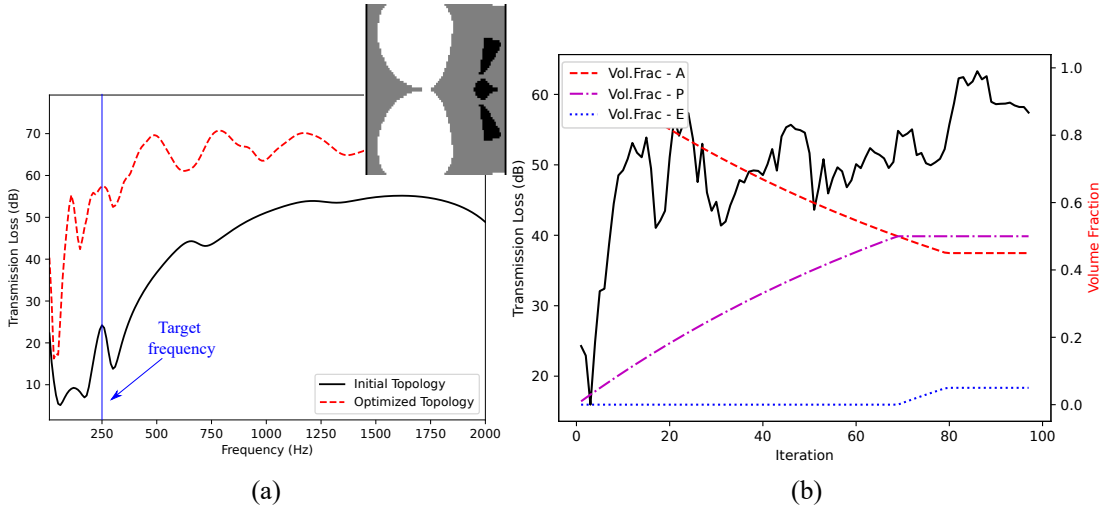

Figure 2 – Main results of the Hard-Symmetry system case, with (a) the transmission loss responses of the initial and final configurations, highlighting the final topology, together with (b) the evolution of the objective function and volume fractions of the three materials under consideration.

All of these findings can also be extended to the SS case (Fig. 3), given that the materials are close together in the resulted topology and the TL enhancements are of 41.67 dB, but with oscillatory evolution. A different point is that, in the HS configuration, both poroelastic and elastic materials seem to be drawn to the left and right sides of the domain, while in the SS scenario these components are mainly located on the top and bottom portions of it. Such behavior is clearly caused by the different boundary conditions considered, in a way that the HS case may represent a superior far end part of a periodic structure (being the hard wall on the top and the periodic boundary on the bottom) and the SS condition may be seen as the body part of said periodic structure (repeating themselves up and down).

CONCLUSIONS

In this work a topology optimization problem was developed, in order to design systems composed of acoustic-poroelastic-elastic elements. Additionally, to ensure that clear design configurations are obtained at the end of the procedure, the BESO method was chosen. In this scenario, transmission loss values were maximized at 250 Hz, while poroelastic and elastic materials were introduced in a design domain initially filled of acoustic elements, hence configuring a multiphase approach. The modeling of such material phases was done by the unified multiphase technique, which made use of Biot's equations, in the mixed $\mathbf{u}/p$, to obtain the scalar Helmholtz and elasto-dynamic expressions.

These fully modeled components were then systematically changed along the optimization iterations by an introduced material interpolation scheme. In this scenario, two problems were investigated, being geometrically similar, but with differences in the boundary configuration. In both cases, the transmission loss values were successfully enhanced and the material disposition kept the components close to each other (with almost no material disconnection). As a drawback, a great deal of variations occurred in the evolution of the objection function due to the iterative step chosen (ER and $\mathrm{AR}_{\mathrm{max}}$

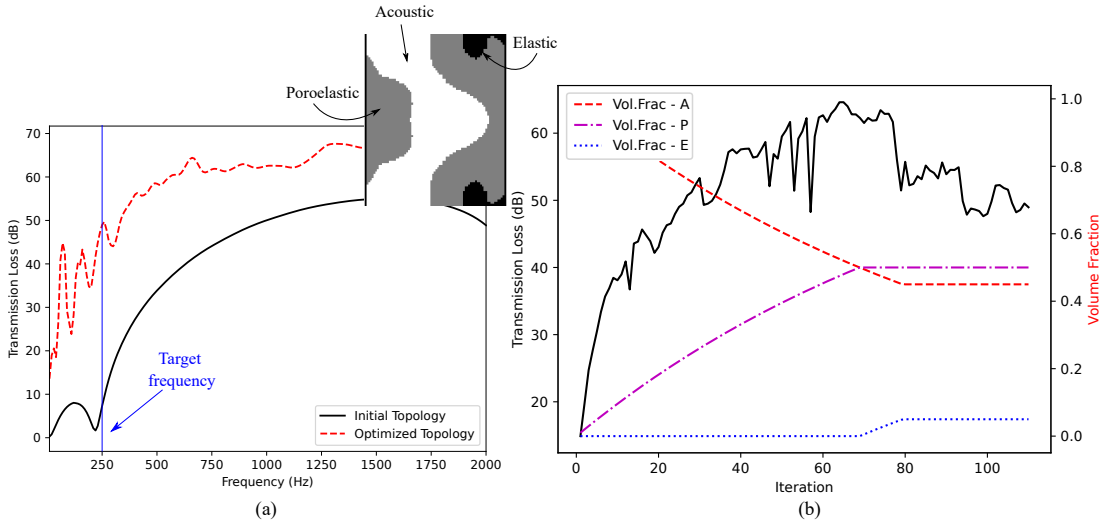

Figure 3 – Main results of the Symmetry-Symmetry system case, with (a) the transmission loss responses of the initial and final configurations, highlighting the final topology, together with (b) the evolution of the objective function and volume fractions of the three materials under consideration.

values).

ACKNOWLEDGMENTS

The authors would like to acknowledge the financial support given by the Fundação de Amparo à Pesquisa do Estado de São Paulo (FAPESP), project numbers 2013/08293-7, and by the Coordenação de Aperfeiçoamento de Pessoal do Nível Superior (CAPES), finance code 001.

REFERENCES

Allard, J.F. and Atalla, N., 2009, "Propagation of Sound in Porous Media: Modelling Sound Absorbing Materials", Ed. John Wiley & Sons, West Sussex, United Kingdom, 358 p.

Atalla, N., Panneton, R. and Debergue, P., 1998, "A mixed displacement-pressure formulation for poroelastic materials", J. Acoust. Soc. Am., Vol. 104, pp. 1444-1452.

Atalla, N., Hamdi, M.A. and Panneton, R., 2001, "Enhanced weak integral formulation for the mixed (u,p) poroelastic equations", J. Acoust. Soc. Am., Vol. 109, pp. 3065-3068.

Atalla, N. and Sgard, F., 2015, "Finite Element and Boundary Methods in Structural Acoustics and Vibration", Ed. CRC Press, Florida, United States, 441 p.

Azevedo, F.M., Moura, M.S., Vicente, W.M., Picelli, R. and Pavanello, R. 2018, "Topology optimization of reactive acoustic mufflers using a bi-directional evolutionary optimization method", Struct. Multidiscip. Optim., Vol. 58, pp. 2239-2252.

Biot, M.A., 1956, "Theory of Propagation of Elastic Waves in a Fluid-Saturated Porous Solid: I. Low-Frequency Range", J. Acoust. Soc. Am., Vol. 28, pp. 168-178.

Biot, M.A., 1956, "Theory of Propagation of Elastic Waves in a Fluid-Saturated Porous Solid: II. Higher-Frequency Range", J. Acoust. Soc. Am., Vol. 28, pp. 179-191.

Champoux, Y. and Allard, J., 1991, "Dynamic tortuosity and bulk modulus in air-saturated porous media", J. Appl. Phys., Vol. 70, pp. 1975-1979.

Ferrándiz, B., Denia, F.D., Martínez-Casas, J., Nadal, E. and Ródenas, J.J., 2020, "Topology and shape optimization of dissipative and hybrid mufflers ", Struct. Multidiscip. Optim., Vol. 62, pp. 269–284.

Hu, J., Yao, S. and Huang, X., 2022, "Topological design of sandwich structures filling with poroelastic materials for sound insulation", Finite Elem. Anal. Des., Vol. 199, pp. 103650.

Huang, X. and Xie, Y.M., 2010, "Evolutionary Topology Optimization of Continuum Structures: Methods and Applications", Ed. John Wiley & Sons, West Sussex, United Kingdom, 223 p.

Johnson, D.L., Koplik, J. and Dashen, R., 1987, "Theory of dynamic permeability and tortuosity in fluid-saturated porous media", J. Fluid Mech., Vol. 176, pp. 379-402.

Lee, J.S., 2009, "Unified Multi-Phase Modeling and Topology Optimization for Complex Vibro-Acoustic Systems Consisting of Acoustic, Poroelastic and Elastic Media", School of Mechanical and Aerospace Engineering, The Graduate School, Seoul National University.

Lee, J.S., Göransson, P. and Kim, Y.Y., 2015, "Topology optimization for three-phase materials distribution in a dissipative expansion chamber by unified multiphase modeling approach", Comput. Method Appl. M., Vol. 287, pp. 191-211.

Lee, J.S., Kang, Y.J. and Kim, Y.Y., 2012, "Unified multiphase modeling for evolving, acoustically coupled systems consisting of acoustic, elastic, poroelastic media and septa", J. Sound Vib., Vol. 331, pp. 5518-5536.

Lee, J.W. and Kim, Y.Y., 2009, "Topology optimization of muffler internal partitions for improving acoustical attenuation performance", Int. J. Numer. Meth. Eng., Vol. 80, pp. 455-477.

Pereira, R.L., Lopes, H.N. and Pavanello, R., 2022, "Topology optimization of acoustic systems with a multiconstrained BESO approach", Finite Elem. Anal. Des., Vol. 201, pp .103701.

Rigobert, S., Atalla, N. and Sgard, F.C., 2003, "Investigation of the convergence of the mixed displacement-pressure formulation for three-dimensional poroelastic materials using hierarchical elements", J. Acoust. Soc. Am., Vol. 114, pp. 2607-2617.

Yamamoto, T., Maruyama, S., Nishiwaki, S. and Yoshimura, M., 2009, "Topology design of multi-material soundproof structures including poroelastic media to minimize sound pressure levels", Comput. Method Appl. M., Vol. 198, pp. 1439-1455.

Yoon, G. H., 2013, "Acoustic topology optimization of fibrous material with Delany–Bazley empirical material formulation", J. Sound Vib., Vol. 332, pp. 1172-1187.

Zhou, E. L., Wu, Y., Lin, X. Y., Li, Q. Q. and Xiang, Y., 2021, "A normalization strategy for BESO-based structural optimization and its application to frequency response suppression", Acta Mech., Vol. 232, pp. 1307-1327.

RESPONSIBILITY NOTICE

The authors are the only partyies responsible for the printed material included in this paper.